

PAPER • OPEN ACCESS

## Validation of Unsteady CFD considering Thermal Load Fluctuation in Office Room

To cite this article: K Fukada and M Miyata 2019 *IOP Conf. Ser.: Earth Environ. Sci.* **238** 012033

View the [article online](#) for updates and enhancements.

You may also like

- [Study on load characteristics of different air conditioning systems in large space railway station](#)

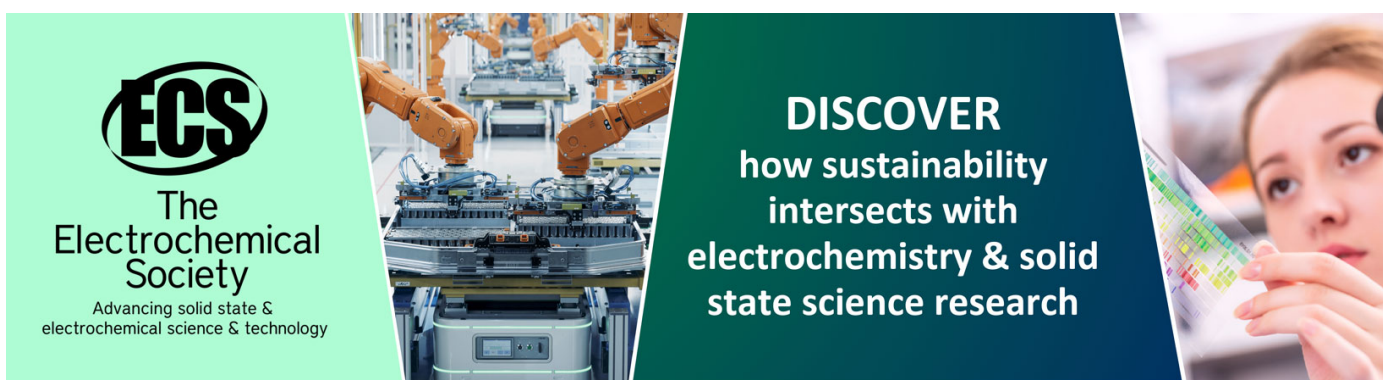
Shan Peng, Jinghua Yu, Wenjie Gang et al.

- [Cost of preventing workplace heat-related illness through worker breaks and the benefit of climate-change mitigation](#)

Jun'ya Takakura, Shinichiro Fujimori, Kiyoshi Takahashi et al.

- [Load Prediction and Control of Capillary Ceiling Radiation Cooling Panel Air Conditioning System Based on BP Neural Network](#)

Gang Pi, Linghong Xu, Qiming Ye et al.



**ECS**  
The  
Electrochemical  
Society  
Advancing solid state &  
electrochemical science & technology

**DISCOVER**  
how sustainability  
intersects with  
electrochemistry & solid  
state science research

# Validation of Unsteady CFD considering Thermal Load Fluctuation in Office Room

K Fukada<sup>1</sup> and M Miyata<sup>2</sup>

<sup>1</sup> SHINRYO CORPORATION, Ibaraki, Japan

<sup>2</sup> National Institute for Land and Infrastructure Management, Ibaraki, Japan

E-mail: fukada.ke@shinryo.com

**Abstract.** In the design stage of air-conditioning equipment, by predicting the annual air-conditioning energy and heat load with high accuracy and by comparing multiple designed air-conditioning systems, it is possible to select optimal equipment and reduce capital investment. However, occasionally, it is difficult to predict energy consumption by means of energy simulation (ES) assuming that the thermal environment of the room is uniform, because of various reasons such as the influence of the uneven distribution of the pieces of equipment that act as heat loads, and mixing loss due to the air-conditioning system. In addition, when evaluating an air-conditioning system considering human comfort in a room, it is necessary to calculate a comfort index such as the Predict Mean Vote (PMV). In that case, it is important to predict the distribution of the thermal environment such as the bias in wall surface temperature. Therefore, attempts have been made to combine Computational Fluid Dynamics (CFD) with energy simulation for predicting the distribution of the thermal environment. However, in a few cases, measurements are made considering thermal load fluctuations in actual outdoor environments, and validation of CFD analysis is performed. Therefore, in this study, in a laboratory simulating an office, considering the effect of actual solar radiation, we measured the performance by changing the air-conditioning system of the perimeter zone and analysed the behaviour of thermal load in the room. Subsequently, by comparing the actual measurement results with the results of unsteady CFD analysis, the prediction accuracy of indoor temperature distribution and air-conditioning heat quantity was validated. As a result, it was clarified that the prediction accuracy of indoor temperature distribution is affected by how the airflow that was directed out of the air conditioner in the perimeter section collides with the window shade.

## 1. INTRODUCTION

When designing air-conditioning equipment, accurately predicting the annual air-conditioning energy requirement and heat load and comparing different system designs can enable optimal equipment to be selected and reduce the capital investment. However, it can sometimes be difficult to predict energy consumption using ES assuming that the thermal environment of the room is uniform, because of various reasons such as the influence of the uneven distribution of the pieces of equipment that act as heat loads and mixing loss due to the air-conditioning system. In addition, when human comfort is a factor in evaluating an air-conditioning system, we also need to calculate a comfort index, such as PMV. In such a case, it is important to predict the distribution of the thermal environment such as the bias at the wall surface temperature. Therefore, attempts have been made to combine ES with CFD programs to predict the distributions of the indoor thermal environments; examples have been



provided by Nielsen and Tryggvason (1998), Zhai and Chen (2003 and 2005). In addition, Iida et al. (2014) applied this approach to an existing office building. However, in a few cases, measurements are performed by considering the thermal load fluctuations in actual outdoor environments, and CFD analysis is validated. In this study, considering the effect of actual solar radiation, we measured the performance of a laboratory simulating an office environment by changing the air-conditioning system of the perimeter zone and analyzed the behavior of the thermal load in the room. Subsequently, by comparing the actual measurement results with the results of unsteady CFD analysis, the prediction accuracy of indoor temperature distribution and the air-conditioning heat quantity were validated. We focused on the simulated office, by considering the effect of actual solar radiation, comparing the air-conditioning system in the perimeter zone, and conducting comparative measurements to understand the behavior of the room's heat load. In addition, we evaluated the accuracy of the indoor temperature distribution and the air-conditioning heat quantity predictions by comparing the measured state of the outside air with the unsteady CFD analysis results. In this way, we aim to contribute to future studies that couple ES and CFD programs.

## 2. MEASUREMENTS

Figure 1 shows an overview of our laboratory, where the furniture was arranged so as to simulate an office. The laboratory is located on the fourth (i.e., top) floor of a four-story building and has windows on the south and east walls. Table 1 shows the measurement conditions. All the walls, ceilings, and floors were insulated with glass wool. During the measurement period, the window shades remained closed all day, at a slat angle of  $45^\circ$ , and the air-conditioning system operated on the schedule shown in Table 1. The air-conditioning system in the interior zone used common ceiling outlets, while the one in the perimeter zone changed each day, with ceiling outlets used on Aug. 19th and the floor-standing packaged air conditioners (PACs) used on the 20th. The interior air-conditioning was controlled by two systems, SA\_I1 on the south side and SA\_I2 on the north side. The ceiling outlets around the perimeter were controlled by three systems, SA\_C1 to SA\_C3, while the floor-standing PACs were controlled by six systems, SA\_F1 to SA\_F6. The air conditioning had been operated at a fixed temperature of  $26^\circ\text{C}$  on the same schedule for more than a week before the measurement period. The room's temperature was measured by type-T thermocouples. As shown in Figures 2 and 3, the vertical temperature distribution was measured at seven points on each of 18 poles, with both the supply air (SA) and return air (RA) temperatures being measured. The surface temperatures of the

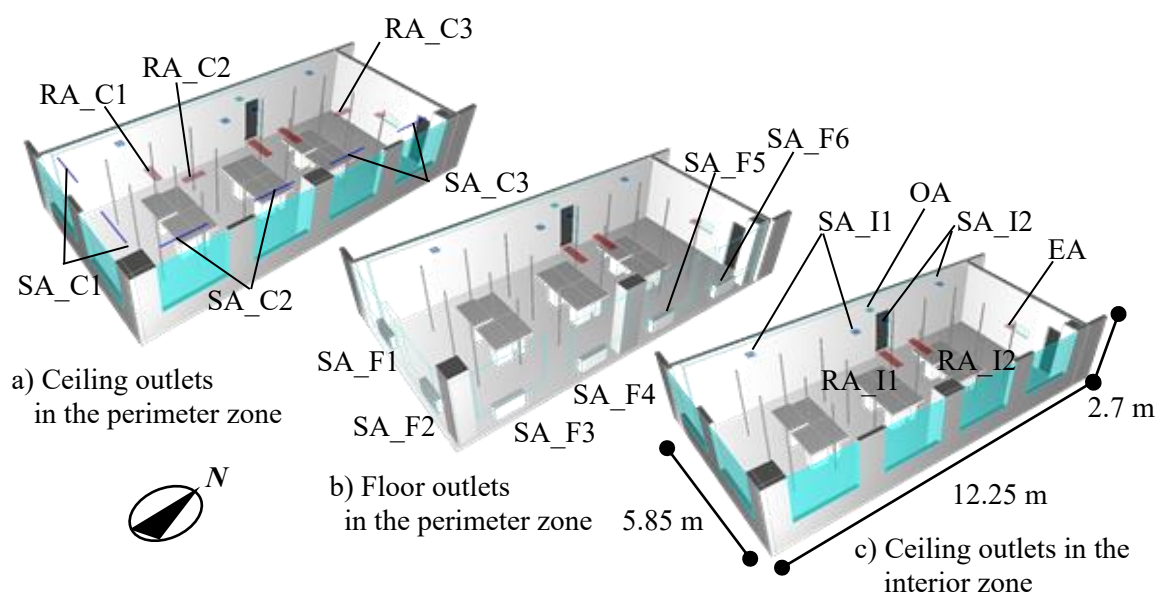


**Figure 1.** Overview of the simulated office.

ceiling and floor were measured by thermocouples at the top and bottom of each pole. The air temperatures in the adjacent room, above the ceiling, under the floor, and outside were also measured. The global solar radiation was measured in the horizontal plane on the rooftop. Heat-flow meters were installed on all the walls, floors, and ceilings, and the surface temperatures of the window shades were measured by a thermal camera.

**Table 1.** Measurement conditions.

Structure specification: Reinforced concrete construction with glass wool insulation (Insulation thickness: ceiling $t = 100\text{mm}$ , wall $t = 50\text{ mm}$ )
Window specification: Float plate glass and low-emissivity double glazing
Air conditioning
Aug. 19 <sup>th</sup> 07:00–20:00: Interior and perimeter air conditioning system (Ceiling outlet type)
Aug. 20 <sup>th</sup> 07:00–20:00: Interior and perimeter air conditioning system (Floor outlet type)
Aug. 21 <sup>st</sup> 07:00–20:00: Interior air conditioning system (Ceiling outlet type)
Design temperature: $26^{\circ}\text{C}$ on all days
Other conditions
Ventilation airflow rate: 07:00–20:00, $12\text{ m}^3/\text{min}$
Lighting load: 08:00–20:00, $640\text{ W}$ ( $27.6\text{ MJ/day}$ )
Equipment load: all day, $118.5\text{ W}$ ( $10.2\text{ MJ/day}$ ), ex. PC, measuring equipment
Shades: closed all day

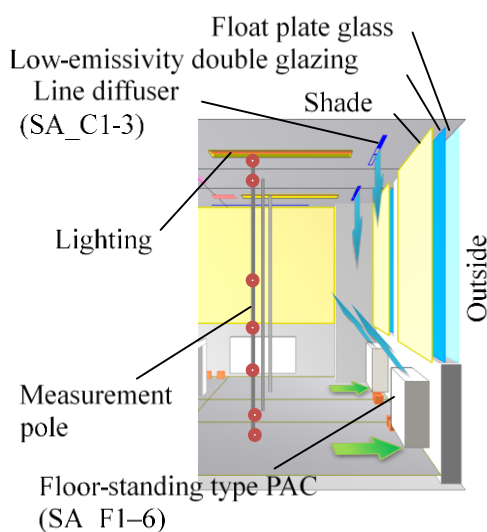


**Figure 2.** Air conditioning system (perimeter).

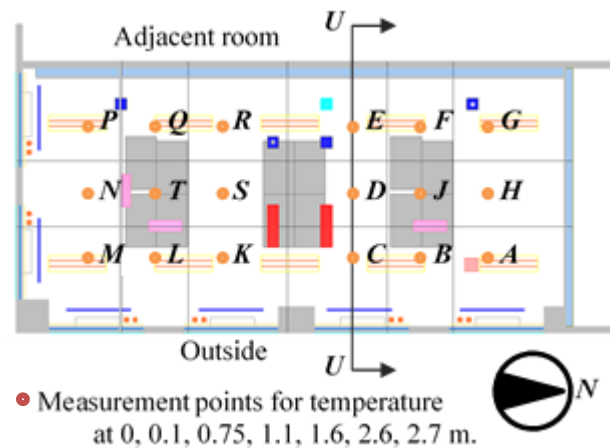


**Figure 3.** Plan of the simulated office.

### 3. CFD ANALYSIS

We also conducted an unsteady CFD analysis for Aug. 19th to 21st to predict the indoor thermal environment. Figure 1 shows the calculation domain, which consisted of 3,644,352 cells. A time interval of 1 s was used for the calculations. We compared the results of this analysis with the measurement results in terms of the RA temperature, transition time of the room's vertical temperature distribution, and the air-conditioning system's daily cooling load. To evaluate the effect of different thermal load boundary conditions on the analysis accuracy, we considered two cases. In Case 1, the

walls' measured surface temperatures were used as boundary conditions, while Case 2 used the measured external temperature and the quantity of direct and sky solar radiation. The CFD analysis was carried out starting 1 week before the measurement period. The analysis was performed using commercial software, namely scSTREAM V11 (Software Cradle Co., Ltd.). We applied the finite volume method, and treated the air as an incompressible fluid using the Boussinesq approximation. In addition, we used the standard k-ε turbulence model and applied the SIMPLEC algorithm, with the QUICK scheme for the advection term. We used an orthogonal structured grid with log law wall boundary conditions, and set the convective heat transfer coefficient to 4.5 W/m<sup>2</sup>·K. We carried out a radiation coupling analysis with view factor calculations. In the solar radiation analysis, we set the short wavelength absorption rate, transmittance, and reflectance of each wall surface and calculated the heat sources on each surface by the view factor method. The window shades were modeled as having zero thickness while considering radiation and heat conduction, and the drag coefficient was

**Table 2.** Air conditioning conditions

Unit	Cooling flow rate [m <sup>3</sup> /min]	Isothermal flow rate [m <sup>3</sup> /min]	Outlet boundary conditions: $k_{in} = U^2/100$ [m <sup>2</sup> /s <sup>2</sup> ], $\epsilon_{in} = 0.09^{3/4} \times k^{3/2}/W$ [m <sup>2</sup> /s <sup>3</sup> ] where $U$ : outlet velocity [m/s], $W$ : shortest outlet length [m]
SA_I1-2	16.5	12.0	Supply temperature: measured for 5 s
SA_C1-3	13.0	8.0	
SA_F1-6	7.0	6.0	

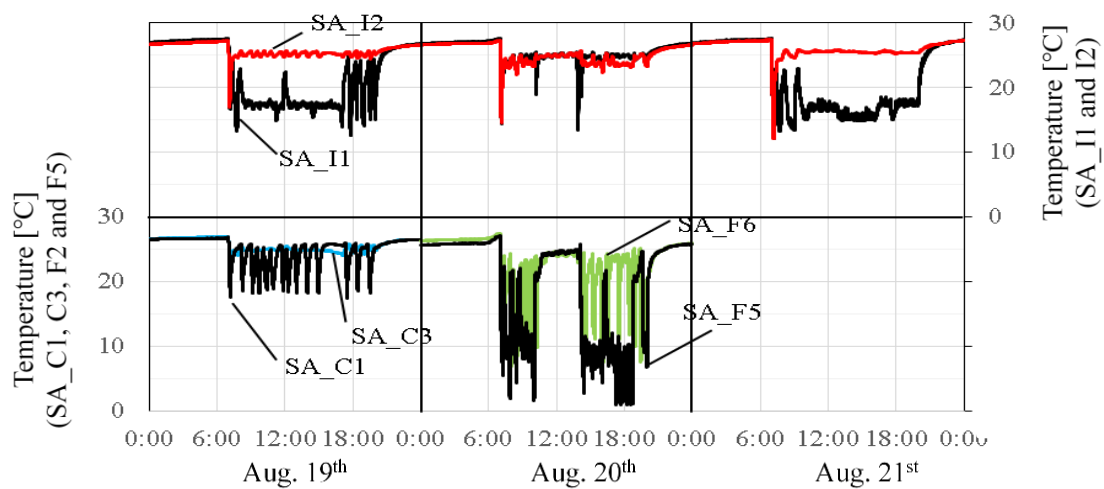


**Figure 4.** Measured supply temperatures. (Upper: SA\_I1 and I2, lower: SA\_C1, C3, F2, and F5)

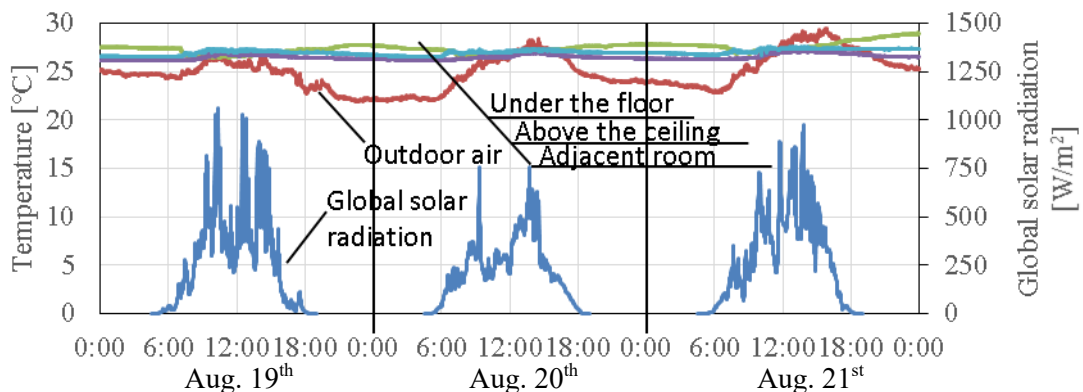


**Figure 5.** Measured global solar radiation and temperature around the office.

set to enable air to flow. Table 2 shows the air-conditioning parameters, based on measuring both the outlet airflow rate and temperature for 5 s. Figure 4 shows the measured supply temperatures at each of the outlets. In Case 1, the window shade surface temperatures were measured every hour, and the wall, ceiling, and floor temperatures were averaged over 10 min. In Case 2, the external temperature was averaged over 10 min, and the solar radiation was averaged over 1 min. Figure 5 shows the external temperature and solar radiation values used for the CFD analysis.

## 4. RESULTS AND DISCUSSION

### 4.1. Daily air conditioner cooling load

Figure 6 shows the measured and calculated temperatures for RA\_I1. On Aug. 19<sup>th</sup>, the measurement and analysis results show almost the same trends, with a difference of about  $\pm 0.5^\circ\text{C}$ . On Aug. 20<sup>th</sup>, the analysis result is lower, by about  $2^\circ\text{C}$ . On Aug. 21<sup>st</sup>, the Case 1 values are almost the same as the measured ones, but without their temperature fluctuations. In Case 2, the calculated values are about  $0.5^\circ\text{C}$  higher than the measured ones after 10:00, but show the same trends. Figure 7 shows the measured and calculated temperatures for RA\_C3, RA\_F5, and the exhaust air (EA). On Aug. 19<sup>th</sup>, the analysis results are about  $1^\circ\text{C}$  lower than the measured values, while on Aug. 20<sup>th</sup>, the analysis results were lower by at least  $2^\circ\text{C}$  (Case 1) or  $1^\circ\text{C}$  (Case 2). On Aug. 21<sup>st</sup>, the differences between the measured and calculated EA temperatures are about  $-1^\circ\text{C}$  (Case 1) and  $+0.5^\circ\text{C}$  (Case 2). Next, Table 3 compares the air conditioners' daily cooling loads, which were calculated from the difference between the measured SA and RA temperatures and the air flow rate. On Aug. 19<sup>th</sup>, SA\_I1 (south) and SA\_C3 (northeast) were performing cooling, while the others were operating isothermally. The predicted cooling loads are 16% less (Case 1) and 6% less (Case 2) than the measured values. On Aug. 20<sup>th</sup>, the internal air conditioners operated isothermally almost all day, while the perimeter ones (SA\_F5 and SA\_F6) were mostly cooling. Both analysis results yielded cooling loads that are about 30% less than

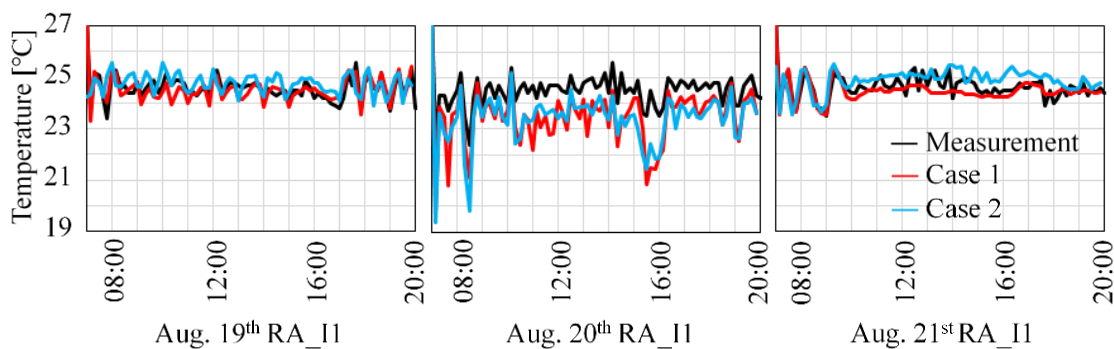


**Figure 6.** Measured and calculated RA temperature: RA\_I1.

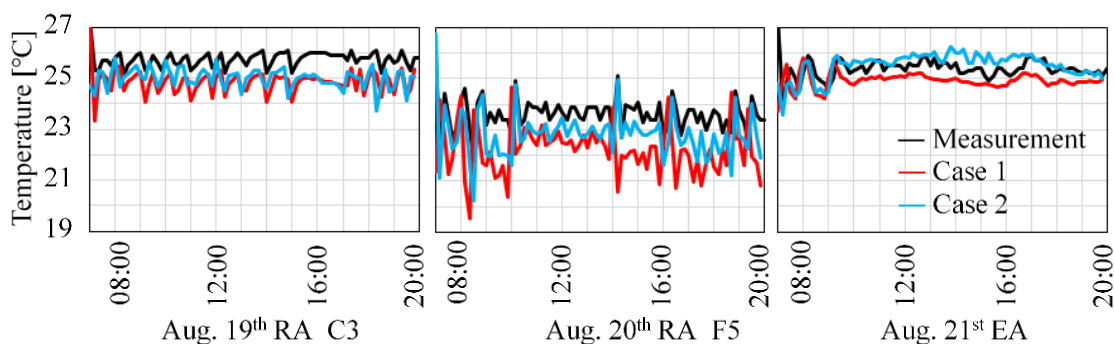


**Figure 7.** Measured and calculated RA (perimeter) and EA temperatures.

the measured values. On Aug. 21<sup>st</sup>, only air conditioner SA\_I1 (south interior) was required for cooling. Here, the predicted cooling loads are 3% less (Case 1) and 9% more (Case 2) than the measured values. Table 4 shows the ventilation and skin loads. The ventilation load indicated a sensible heat load due to taking outside air. The skin load was calculated by subtracting the ventilation load and equipment heat load (37.8 MJ/day) from the cooling load. On Aug. 20<sup>th</sup>, the predicted ventilation load is 20% higher than the measured value, but the predicted skin load is less than half of the actual value. On Aug. 19<sup>th</sup> and 21<sup>st</sup>, the predicted and measured values are very similar. The global solar radiation measurements on each of the three days are 13.7, 11.6, and 14.5 MJ/m<sup>2</sup>, so the radiation was lowest on the 20<sup>th</sup>. We therefore believe that the amount of solar radiation received from the window and shade surfaces increased due to the outlet air flow from the floor-standing PACs. Furthermore, when we compare the skin loads on the 19<sup>th</sup> and 21<sup>st</sup>, it is higher on the 19<sup>th</sup>, when the solar radiation was highest, implying that directly air-conditioning the perimeter increases the solar heat gain.

**Table 3.** Measured and calculated daily air conditioner cooling loads.

	Aug. 19 <sup>th</sup> [MJ/day]						Aug. 21 <sup>st</sup> [MJ/day]		
	I1	I2	C1	C2	C3	Total	I1	I2	Total
Measurement	-93.1	5.2	2.3	2.4	-20.2	-103.4	-112.0	6.9	-105.1
Case 1	-91.6	6.0	5.8	5.8	-12.6	-86.5	-110.3	8.0	-102.3
Case 2	-94.2	3.6	2.3	4.4	-13.6	-97.5	-115.9	0.9	-115.0
	Aug. 20 <sup>th</sup> [MJ/day]								
	I1	I2	F1	F2	F3	F4	F5	F6	Total
Measurement	-0.2	-3.5	-37.1	-17.2	-3.7	-32.5	-52.1	-60.4	-206.7
Case 1	10.4	9.6	-29.8	-13.3	0.3	-28.6	-44.6	-49.5	-145.4
Case 2	13.0	15.4	-30.5	-13.2	0.1	-28.1	-47.1	-53.0	-143.4

**Table 4.** Measured and calculated daily ventilation and skin loads.

	Ventilation load [MJ/day]			Skin load [MJ/day]		
	Aug. 19 <sup>th</sup>	Aug. 20 <sup>th</sup>	Aug. 21 <sup>th</sup>	Aug. 19 <sup>th</sup>	Aug. 20 <sup>th</sup>	Aug. 21 <sup>st</sup>
Measurement	25.5	44.3	37.1	40.0	124.6	30.1
Case 1	25.6	53.6	43.6	23.0	53.9	20.8
Case 2	23.0	52.4	35.3	36.6	53.0	41.9

#### 4.2. Room temperature distribution

Figure 8 shows the measurement and analysis results for the vertical temperature distributions of poles C (perimeter) and J (interior) during Aug. 19<sup>th</sup> to 21<sup>st</sup>. These show the same trends on both the 19<sup>th</sup> and 21<sup>st</sup>, to within 1°C. On the 20<sup>th</sup>, however, there is a large discrepancy in the results for Pole C, with the predicted values being around 2°C lower. In particular, at 08:30 (while the room was being cooled), the temperature is lowest near the ceiling, with discrepancies of 3°C (Case 1) and 2°C (Case 2). Figure 9 shows the predicted temperature and wind velocity distributions for Section U in Case2, which includes Pole C. Both cases show cool outlet air flowing along the ceiling and toward the center of the room. Given this, we believe that the larger predicted ventilation load shown in Table 4 is due to a flow of cool air (cooler than the actual temperature) coming from the exhaust port on the ceiling. Figure 10 shows the indoor temperature distribution over time (Pole J, 1.1 m from the floor). On the

19<sup>th</sup> and 21<sup>st</sup>, the analysis results are about 1°C lower, but show almost the same trends. On the 20<sup>th</sup>, the analysis results differ by 2°C, but rise slowly after 14:00 in Case 1. One factor in these results is that, although the surface temperatures were used as the boundary conditions, the thermal camera only acquired data once an hour, so it could not capture the sudden temperature rise of the window shade due to solar radiation.

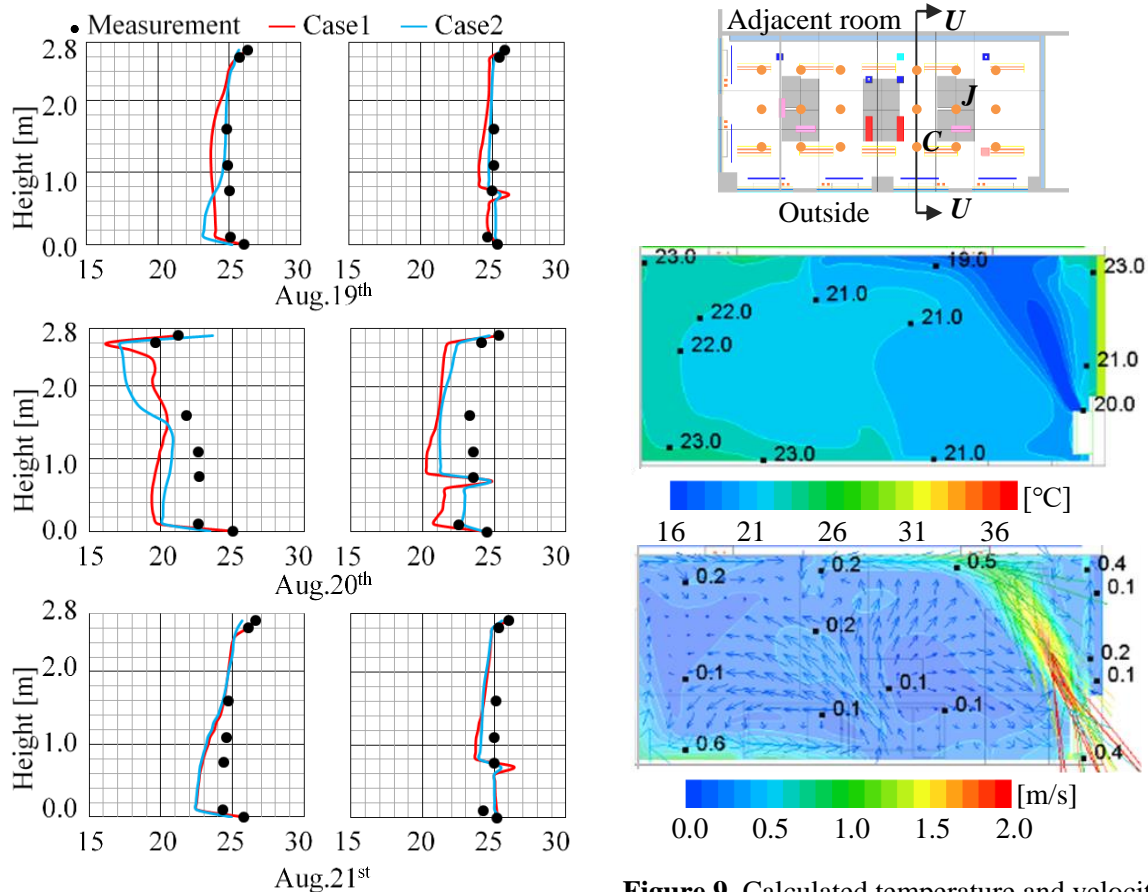


**Figure 8.** Measured and calculated vertical air temperature distributions at 8:30.

**Figure 9.** Calculated temperature and velocity distributions at Section U in Case2. (Aug. 20<sup>th</sup>, 08:30)

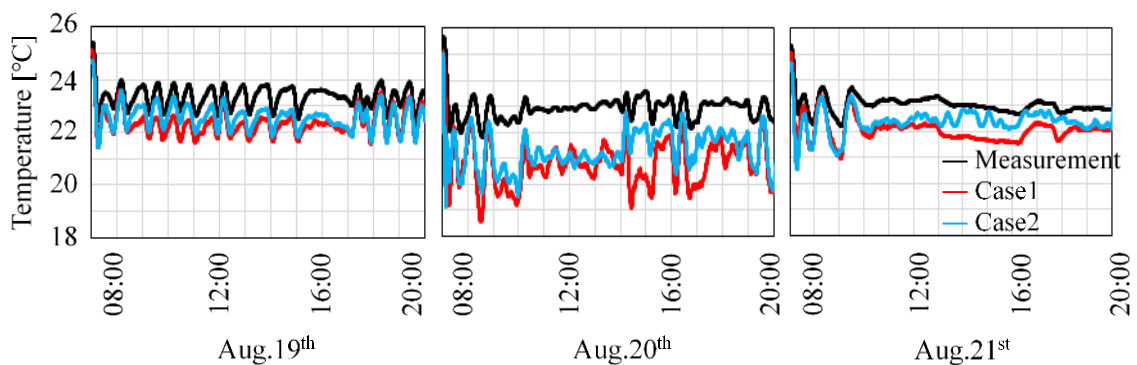


**Figure 10.** Measured and calculated temperatures over time. (Pole J, 1.1 m from floor)

## 5. CONCLUSION

In our laboratory simulation of an office, we measured the indoor thermal environment and cooling load by changing the air-conditioning system in the perimeter zone and compared the results with the results of CFD analysis. From this, we discovered the following. The CFD analysis reproduced the trends in the RA, indoor temperature, and cooling load to within  $\pm 10\%$  by using measured outdoor environment values. In addition, using both the wall surface temperatures and the conditions around the laboratory as boundary conditions gave almost the same results. However, when the perimeter zone was conditioned by floor-standing PACs, there was a large difference between the predicted and measured skin loads. Given this, the CFD analysis accuracy may be significantly reduced depending on how the air-conditioning system interacts with the window surroundings. In future work, we plan to study a simplified modelling method around windows to increase the accuracy of the solar heat gain predictions considering the accuracy of CFD analysis and computational work in coupling the ES and CFD program, .

## REFERENCES

- [1] Nielsen P V and Tryggvason T 1998 Computational Fluid Dynamics and Building Energy Performance Simulation, *Proceeding of ROOMVENT'98 (Stockholm)* vol 1 pp 101-107
- [2] Zhai Z and Chen Q 2003 Solution characters of iterative coupling between energy simulation and CFD programs *Energy and Building* **35** pp 493-505
- [3] Zhai Z and Chen Q 2005 Performance of coupled building energy and CFD simulations *Energy and Building* **37** pp 333-344
- [4] Iida R, Tomiyasu Y and Shiraishi Y 2014 Commissioning of Air-Conditioning System Using Natural Ventilation in an Office Building Part 2-Performance Evaluation by Coupled Simulation of Building Energy Simulation Tool and Unsteady CFD Analysis *SHASE Transaction* **40(216)** pp 27-35